International Journal of Engineering Research and Advanced Technology (IJERAT)

DOI: 10.31695/IJERAT.2019.3388

E-ISSN : 2454-6135

Volume.5, Issue 2
February -2019

Spatio-temporal characterization of Agricultural Drought using Soil Moisture Deficit Index (SMDI) in the Upper Tana River basin, Kenya

Raphael Muli Wambua[1*]

[1]Department of Agricultural Engineering

Egerton University

Kenya

ABSTRACT

Occurrence of Agricultural drought in a river basin is associated with food insecurity. There is need to integrate agricultural drought characteristics in decision making within upper Tana River basin. In this research, characterization of spatio-temporal Agricultural Drought using Soil Moisture Deficit Index (SMDI), based on hydro-meteorological data was conducted. Eight meteorological stations with data for 41 years were used. The computation was interpolated using kriging interpolation technique within ArcGIS environment. The long-term soil-water was simulated using AquaCrop model. For station ID 9037112, the values of SMDI for dry season are lower than those for the wet seasons. It is deduced that the lower elevations of the basin in south-eastern parts exhibit more drought-prone areas than those in the higher elevations at north-western areas. From this study, Severity-area-frequency curves (SAF) curves for 2, 5, 10, 20, 50 and 100-year return periods were developed. The analysis of spatio-temporal drought characteristics can be adopted for prioritized mitigation of agricultural drought impacts.

Key words: *SMDI, AquaCrop model, Upper Tana River basin, SAF curves.*

1. INTRODUCTION

Significant research has been conducted in water resources and hydrology but drought research is still inadequate in many river basins in the world. Agricultural drought is an event associated with low food production and or food insecurity in an area [1] and [36]. Agricultural drought refers to the deficit of soil moisture due to meteorological effects with different timing and effects. This drought depends upon soil moisture deficit [2], [33], water storage capacity of the soil and the hydro-meteorological variables. Since the drought is characterized by deficit of soil moisture content in the soil which is usually required by plants, it adversely affects any vegetation and or crop grown on land [3], [36], and [14].

Agricultural drought can be monitored by assessing soil moisture content levels. However, direct soil moisture data measurement is not available at regional and basin scales. To estimate soil moisture content, process-based models may be used. In such models, an integration of both the random variables of climate and physical properties of land are considered. One of the advantages of these models is that they can be used to provide information at different spatial and temporal resolutions. Some of these process-based models include the FAO developed AquaCrop model [5] and Soil and Water Assessment Tool (SWAT) [10]. The Aquacrop model has been used in modelling crop response to soil water availability in a number of studies. For instance, AquaCrop model was applied to evaluate wheat grain yield and crop biomass in China for irrigation systems [8]. It was also applied by [12] to assess crop grain yield and biomass response to soil water content and actual evapotranspiration under deficit irrigation conditions.

There are two broad categories of drought indices; satellite based and the data driven drought indices [2]. The satellite or Remote Sensing (RS) indices involve the application of the science and art of obtaining information of points, objects, areas or phenomena through analysis of data acquired by a sensor, which is not in direct physical contact with the target of investigation [34]. On the other hand, the Data Driven Drought Indices use a single or a combination of hydro-meteorological variables as input parameters to assess drought intensity, duration, severity and magnitude. The two broad types of droughts may further be grouped into four main categories of droughts according to [43]. These include the Hydrological, Meteorological, Agricultural and Socio-economic droughts. The first three types are called the operational droughts and can be integrated into a drought management algorithm. Their relation can then be applied in development of water resource strategy in a river basin [16]. Propagation of hydrological and agricultural drought originates from meteorological droughts which develop from changing phenomena within the hydrological cycle.
The three operational types of droughts are interconnected. For instance, Agricultural drought links meteorological and/or hydrological drought to agricultural impact. Agricultural droughts impact negatively on farming systems whenever they occur.

Their impacts are normally two-fold; environmental and economic impacts. The agricultural drought is associated with low agricultural production, increased food insecurity, decline in output from agro-processing industries and unemployment incidents in the agricultural sector. From the environmental perspective, agricultural drought is caused by insufficient precipitation, high temperature that causes elevated rates of evapo-transpiration, increased salt concentration in the crop root zones and soils within irrigation systems [21]. The term environmental drought is sometimes used to address the adverse effects of extremely low flows on ecosystems, and may be analysed in the emerging fields of eco-hydrology.

Some of the most critical elements of drought which are used for the design of water storage systems to cope with drought impacts include; longest duration, largest severity, highest intensity and spatial and temporal variation of droughts [19]. Drought duration, severity and intensity are fundamental characteristics of any drought event. Drought duration refers to any continuous period of the sequence with deficit, while intensity is the magnitude below a truncation level. Severity is the cumulative deficit below a truncation level during drought period and may mathematically be defined as the product of the drought intensity and duration. For better understanding of drought characteristics, assessment of the influencing variables is paramount. The statistical analysis for stream flow and precipitation as drought variables include parameters such as: the mean, coefficient of variation, log-1 serial correlation coefficient and the probability distribution function of the sequence under study. The extreme values of drought which include; duration, severity and intensity may be modelled with reference to a certain truncation level. The truncation level is usually taken as the long-term mean of the drought variable [7].

A lot of research has been done in development of different categories drought indices. For instance surface water supply index (SWSI), Stream flow Drought Index (SDI), Standardized precipitation Index (SPI), Effective Drought Index (EDI), Palmer drought severity index (PDSI) and the Soil moisture deficit index (SMDI) are categorized as shown in Table 1. The SMDI is categorized as an agricultural drought as applied in this study.

Table 1: The typical categories of different drought indices

Drought index	Drought type for which the index is adopted
SWSI	Hydrological
SDI	Hydrological
SPI	Meteorological
EDI	Meteorological
SMDI*	Agricultural
PDSI*	Agricultural/Hydrological

*Index is adopted for agricultural drought assessment in this study

Agricultural drought has become more frequent and severe in the Tana River basin lead to food insecurity. There is need to understand the drought so that decision makers can integrate drought characteristics in policy making. In this study, agricultural drought characterized by abnormal water deficiency as detected by SMDI is described. The objective of this research was to characterize spatio-temporal conditions of Agricultural Drought using Soil Moisture Deficit Index (SMDI) in the Upper Tana River basin, Kenya based on hydro-meteorological data for 1970 to 2010.

2. MATERIALS AND METHODS

2.1 Study area

The upper Tana River basin with an area of 17,420 km^2 presented in Figure 3.1 was used for this study. The upper Tana River basin originates from the eastern slopes of Mount Kenya and Aberdares range and is a crucial basin that exhibit different agro-ecological zones in Kenya and very important in regulating the hydrology downstream [11].

The upper Tana River basin lies between latitudes 00° 05' and 01° 30' south and longitudes 36° 20' and 37° 60' east. The downstream ecosystem depend on the upper tana river basin making it a very important basin [28]. The basin drains nine counties in Kenya namely; Muranga, Nyandarua, Kiambu, Kirinyaga, Laikipia, Machakos, Nyeri, Embu and Kitui [40]. The basin is part of a larger area that presents major tributaries of Tana River whose total length from the source to the Indian Ocean is approximately 1,000 km [11]. The Tana River tributaries originate from the slopes of Mount Kenya and Aberdares range. This basin is a principal resource in Kenya since it is critical in water supply, hydro-power generation and agricultural production.

DOI : 10.31695/IJERAT.2019.3388

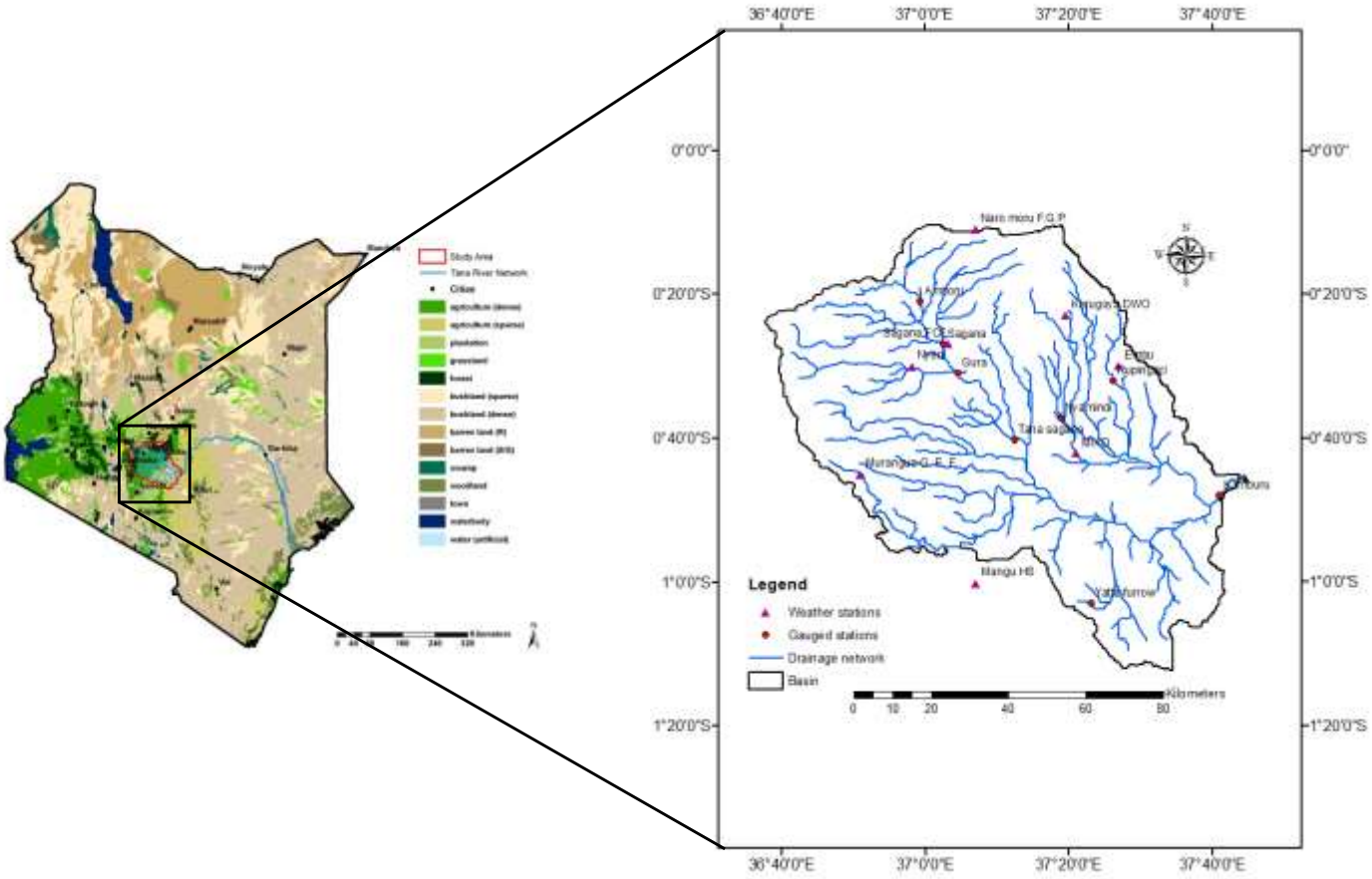

Figure 1: Map of the upper Tana River basin

The elevation of the upper Tana River basin ranges from approximately 730 m to 5,190 m above mean sea level (a.m.s.l.). These elevations are adjacent to Kindaruma hydropower dam and at Mount Kenya respectively which fall within the study area. The River basin exhibits heterogeneous soil types. For instance, Andosols are the soil types which are predominant at higher elevations, Nitosols are at the middle elevations while Ferrasols and Vertisols are at the lower elevations [13].

Precipitation and temperature vary across the river basin. The Mount Kenya and Aberdares ranges receive approximate annual rainfall of 1800 mm (Otieno and Maingi, 2000). Within the middle elevation of 1200 to 1800 m a.m.s.l., the annual rainfall ranges from 1000 to 1800 mm while the lower elevations that are less than 1000 m, receive annual rainfall of 700 mm (Figure 2).

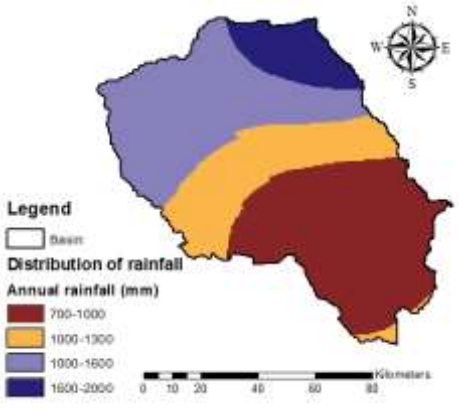

Figure 2: Spatial distribution of annual precipitation in the upper Tana River basin

Although the basin receives significantly high rainfall amounts, it is characterized by seasonal rainfall fluctuations. Generally the basin experiences a bimodal rainfall pattern caused by inter-tropical convergence zone [39]. The rain seasons within the basin are distributed in the months of March to June, and September to December. The precipitation is highly influenced by the orographic forces [32]. The maximum and minimum mean annual temperature vary from 25.5 to 31.0°C and 21.0 to 24.0°C respectively [24]. The average catchment evapo-transpiration is 500 mm in the peak area. There are different land use types in the upper Tana River basin. The main land uses are forests, crop land and range land.

2.2 Data acquisition

DOI : 10.31695/IJERAT.2019.3388

Hydro-meteorological data acquisition

Different data sets were used for this study to compute the SMDI and the drought forecasting models. These data include; stream flow, storage dam levels, precipitation, potential evapo-transpiration, soil moisture content and temperature. The hydro-meteorological data from 1970-2010 (41 years) were used in this study. Part of this data was available while the missing data was estimated for all variables. The available data was on daily time step but had to be re-organized into monthly average time scales for all the variables to match with the data requirements of the present research. The daily stream and monthly flow data was obtained from the Ministry of Environment and Natural Resources, and Water Resources and Management Authority (WRMA).

2.3 Stream flow data

There were fourteen hydrometric stations in the upper Tana River basin with complete and incomplete data records. However, only eight stations were selected for this study since they have sufficient long and reliable data for the period 1970-2010 as required by this study. The stations were in addition considered to be representative of the basin as they are located within the low, lower middle, middle and higher elevations for different agro-ecological zones as required in the study. The station names and gauge identification (ID) numbers, their geographical locations are shown in Table 2. In the present study, only the Masinga dam levels were used because of the availability of long-term data records.

Table 2: Stream flow gauge stations

S.No	Hydrometric Name	Gauge ID	Coordinates	
			Easting	Northing
1	Amboni	4AB05	36.989	-0.350
2	Sagana	4AC03	37.043	-0.449
3	Gura	4AD01	37.076	-0.517
4	Tana sagana	4BC02	37.207	-0.672
5	Yatta furrow	4CC03	37.361	-1.094
6	Nyamindi	4DA10	37.317	-0.621
7	Rupingazi	4DC03	37.438	-0.533
8	Kamburu	4ED01	37.683	-0.800

2.4 Precipitation data

In the upper Tana River basin, data from twenty four meteorological stations were obtained from the Ministry of Water and Irrigation. These stations provided meteorological; precipitation, temperature, evaporation data. The data were then subjected to exploratory data processing. It was found out that only eight stations had reliable and sufficient data. Where the available data contained less than 20% data gaps, then these data were selected for computation the drought soil moisture deficit index (SMDI). The eight stations used in the present study (Table 3) were also objectively located within the low (LE), lower middle (LME), middle (ME) and high (HE) elevations. The stations are located in areas that represent different agro-ecological zones of the basin.

Table 3: Meteorological stations

S.No	Station name	Station ID	Coordinates		Elevation (m)
			Longitude (Degrees)	Latitude (Degrees)	
1	MIAD	9037112	37.350	-0.700	1246
2	Embu	9037202	37.450	-0.500	1494
3	Kerugoya DWO	9037031	37.327	-0.382	1598
4	Sagana FCF	9037096	37.054	-0.448	1234
5	Nyeri	9036288	36.970	-0.500	1780
6	Maragua G. E. F.	9036212	36.850	-0.750	2296
7	Naro-moru F.G.P.	9037064	37.117	-0.183	2296
8	Mangu HS	9137123	37.033	-1.100	1630

2.5 Consistency test of the hydro-meteorological data

A double-mass curve was fitted for the collected hydro-meteorological data to test for its consistency. The consistency of stream flow time series data was conducted to detect for any possible errors resulting from the data measurements. In addition, consistency was used to check for the fluctuations due to climate and weather changes. The cumulative total stream flow and precipitation were computed for each station and then plotted against the cumulative total of an adjacent station. Any sudden change in the gradient of the double-mass curve was considered as an indicator of inconsistency in the data. There was insignificant changes in some station curves and this was neglected thus the data was considered to be consistent.

2.6 Filling in missing data

The continuity of the data records was first examined. It was found out that the meteorological stations; 9037064, 9037112, 9037031, 9137123, 9037202, 9037096, 9036288 and 9036212 (Table 1) had continuous data for 26, 28, 35, 32, 40, 35, 40 and 23 years respectively. The data for each station was partitioned into training and validation data sets comprising 70% and 30% respectively of the total continuously recorded data.

In this study, the ANN structure for each station was obtained by considering different input neurons for different time delays; *t, t-1, t-2,…,t-n,* in the input layer. The number of input variables was equal to the input neurons. The initial number of hidden

DOI : 10.31695/IJERAT.2019.3388

neurons of the ANN model architecture was determined using the procedure adapted from Belayneh (2012) where the hidden layer neurons were initially set at $2n+1$ where n is the input neurons. The Hidden Neurons (HN) were then increased and decreased through trial and error technique for data sets at each hydrometric station. This resulted to an output that was taken as the estimated variable. The ANN model at each station was trained using different ANN.

The output layer comprises neurons in all the networks that are equal to the following month's variable value (I_{t+1}). In this study, the Feed Forward Neural Network (FFNN) and Recursive Neural Network (RNN) were applied and tested in the model training. Initially three different training algorithms were applied to train the structures. These were the back-propagation (BP), Levernberg-Marquardt (LM) and Conjugate Gradient (CG) algorithms. From preliminary results, it showed that a three-layer feed forward neural network with different input and hidden neurons was superior in performance, and that the best results were also obtained using the LM training algorithm. Thus the best ANN structure of three-layer feed forward network based on LM training algorithm was adopted for filling in of missing data in this study. The data was first normalized at each station before exporting it into the graphical user interface (GUI) of the MATLAB. This was done by applying the function given in Equation (1) adapted from [22].

$$X_n = X_{\min} + \frac{(X_o - x_{\min})}{(x_{\max} - x_{\min})} \times (X_{\max} - X_{\min}) \quad (1)$$

Where, X_n = normalized value

X_{min} = the selected minimum value for standardization

X_{max} = the selected maximum value for standardization

X_o = original value

x_{min} = minimum value present in the original data set

x_{max} = maximum value present in the original data set

All the input and output values for ANN were normalized to range between X_{min} of equal to 0.1 and X_{max} of less than 1. According to [22], the values of the X_{min} 0.1 and X_{max} of 0.9 perform best for drought indices such as SPI and EDI. Thus these values were adapted for this study.

After normalization, the various drought forecasting ranges were determined. For each of the ANN model run on the GUI of the MATLAB performance was evaluated based on the correlation coefficient R and Mean Square Error (MSE) criteria and the best model results were selected. The best ANN models were then adopted for filling any missing data for respective meteorological stations. The steps that were followed in filling the missing data are summarized in Figure 3.

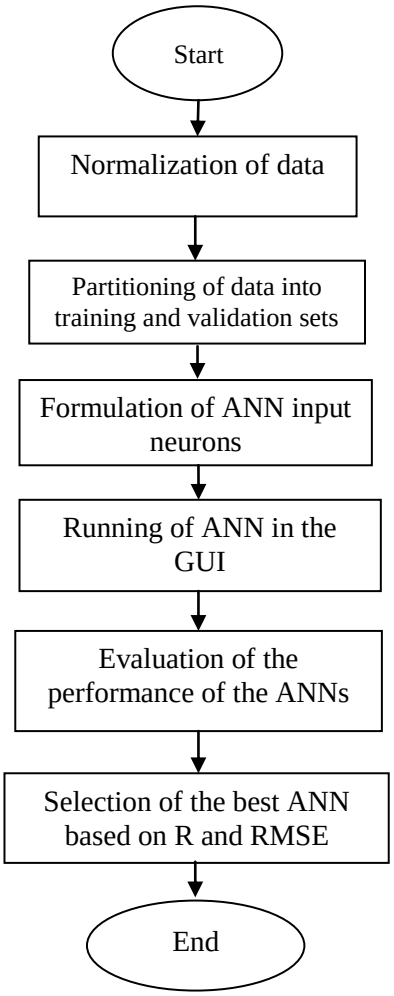

Figure 3: Flow chart of the steps used in filling the missing data using ANN

DOI : 10.31695/IJERAT.2019.3388

2.7 Computation of Soil Moisture Deficit Index

The first step was the preparation of all the AquaCrop input data. The data set consisting of monthly precipitation, maximum and minimum temperature, relative humidity, mean wind speed and sunshine hours for the period 1970-2010 were used for the selected meteorological stations. In addition, soil texture data and 60-cm soil depth profile were used. The 60-cm soil depth was chosen in this study because it represents the most active plant root-zone that contributes to evapo-transpiration process. The 60-cm soil depth represents the potential of most agricultural crops to extract water from rooting depth and according to [9], the quantity of water extracted was considered to depend upon the stage of growth and crop type.

To effectively assess the agricultural drought, data was segregated into dry and wet seasons for specific agricultural applications. This is because different seasons exhibit different drought characteristics as stated by [25], and [37]. Each season had two distinct period with the dry season represented by the period from the months of July to September (J-S), and January to March (J-M). The wet season was represented by the period from October to December (O-D), and March to June (M-J).

2.8 Simulation of Soil Water (SW) content using AquaCrop model

The Input climatic data (average monthly rainfall, maximum temperature (T_{max}), Minimum temperature (T_{min}) and radiation were prepared in excel. First the T_{max}, T_{min} and the radiation data was imported into AquaCrop model where potential evapotranspiration (ET_o) was estimated using Hargreaves method adapted from [35] given as:

$$PE = 0.0023 \times R_a \times (T_{mean} + 17.78) \times (T_{\max} - T_{\min})^{0.5} \quad (2)$$

Where, PE = potential evapotranspiration (mm/month)
R_a = solar/extra-terrestrial radiation (MJ m^{-2} $month^{-1}$)
T_{mean} = mean monthly temperature (^oC)
T_{max} = maximum monthly air-temperature (^oC)
T_{min} = minimum monthly air-temperature (^oC)

The Hargreaves technique was chosen over other methods of estimating ET_o because it requires only temperature and radiation as input data which were available in the study area. After computation of the ET_o, the monthly data sets; the ET_o, dominant soil type and the 60-cm soil depth profile were imported to FAO developed AquaCrop model Version 4.0. The monthly soil water content (SW_i) was then generated from the AquaCrop model. The resulting SW_i was then used to compute $SMDI$ by first calculating the monthly Soil Defict (SD_i) and then $SMDI_i$. Equations (3), (4) and (5) adapted from [27] and [31] were used to estimate the $SMDI$ for the upper Tana River basin.

$$SD_i = \left(\frac{SW_i - MSW_i}{MSW_i - SW_{\min i}} \right) \times 100, \quad for\, SW_i \le MSW_i \quad (3)$$

$$SD_i = \left(\frac{SW_i - MSW_i}{SW_{\max i} - MSW_i} \right) \times 100, \quad for\, SW_i > MSW_i \quad (4)$$

Where, SD_i = soil water deficit (percentage)
SW_i = mean monthly available soil water in a soil profile (mm)
MSW_i = long-term median available soil water in the soil profile (mm)
SW_{maxi} = long-term maximum available soil water in the soil profile (mm)
SW_{mini} = long-term minimum available soil water in the soil profile (mm)

Based on the SDj the SMDI was then computed as:

$$SMDI_j = 0.5 \times SMDI_{j-1} + \frac{SD_j}{50} \quad (5)$$

Where, $SMDI_i$ = soil moisture deficit index for j^{th} week
i = i^{th} month of the year
$SMDI_i$ = the soil moisture deficit for i^{th} month week
SD_i = soil moisture deficit (%) for i^{th} month of a particular year

The integration of all the steps used in computing the values of SMDI are summarized in Figure 4

DOI : 10.31695/IJERAT.2019.3388

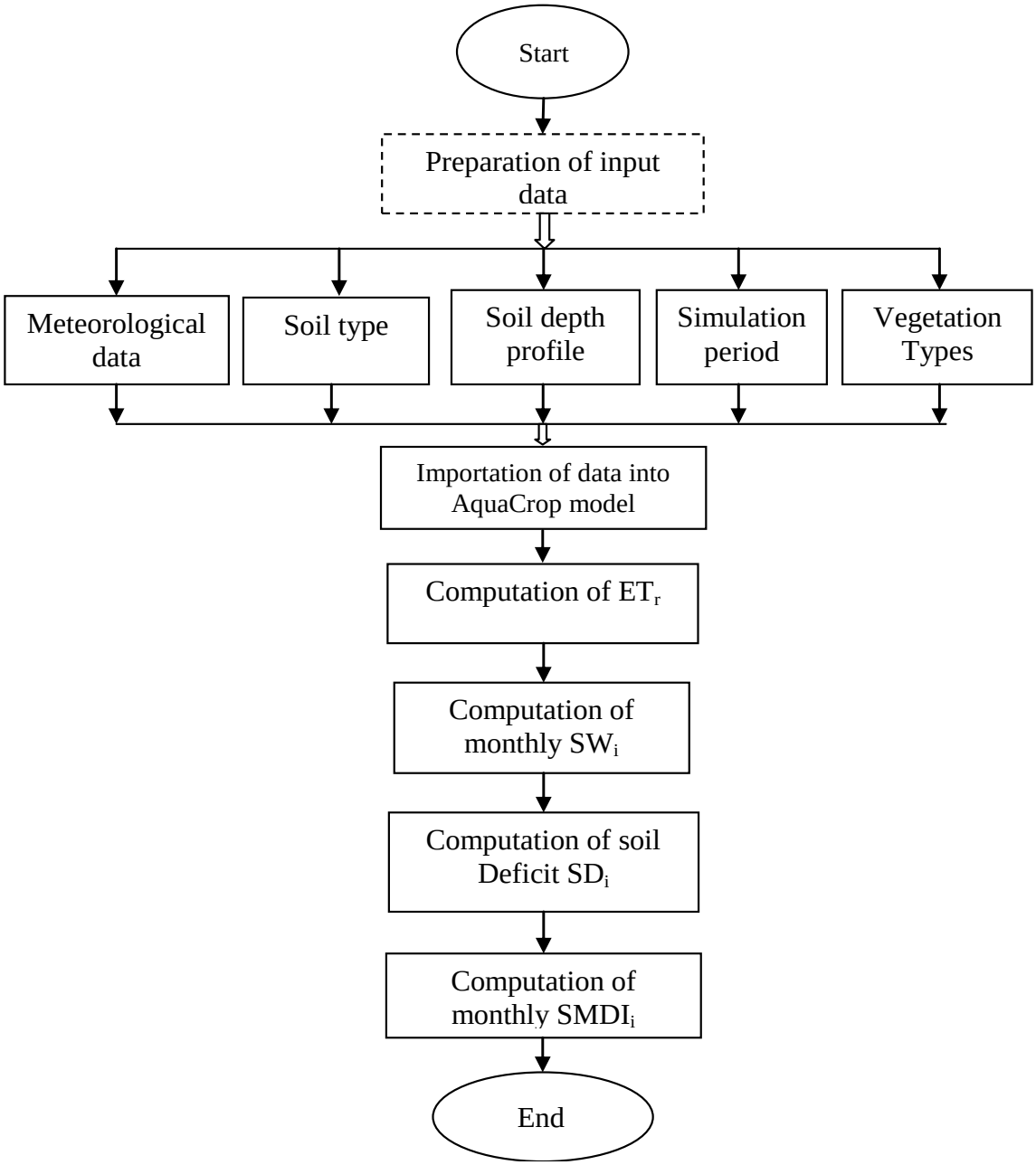

Figure 4: Flow chart showing the steps in computation of SMDI

Future meteorological events can be projected. Recursive multi-step neural networks (RMSNN) with multiple neurons in the input and hidden layers adapted from [20] was used for drought projection from the year 2010 to 2099. The RMSNN consist only of a single neuron in the output layer which represent a one month lead time projection and done for k months (k=1068) . Based on the available data period of 1970 to 2010, the RMSNN was first designed and calibrated considering only one month lead time based on present and several months of the past SMDI values as inputs. The resulting network with the same number of input combination/variables was then used for projecting SMDI values for multiple lead times recursively.The drought projection was conducted at month *t* for *k* time steps from (*t+1*) to (*t+k*). The projection (*t+1*) was first calculated based on n months of the past SMDI values including the NDI at *t*. This projected value $SMDI_{(t+1)}$ was then used with past SMDI values of *t, t-1,…,t-n* months to project $SMDI_{(t+2)}$. This process was repeated recursively to obtain the drought projection for 1068 months to represent the total period from the year 2011 to 2099. By using the projection it is assumed that the drought trend and associated meteorological variables within the basin is the same both for the data period (1970 to 2010) and the projection period (2011 to 2099)

2.9 Spatial distribution of drought severity

The sum of drought severity DI_d values below zero during each year for the study period was calculated. The probability *P* of drought occurrence was determined by dividing the number of months that had *DI* values less than zero by 12 months of the year. The drought severity was then computed at each station using the relation:

$$S = \sum_{N=1}^{N} SMDI_d \times P \qquad (6)$$

Where, *S* = annual drought severity for a defined year

$SMDI_d$ =The *sum* of drought severity values below zero during a particular year

P = probability of drought occurrence for the defined year

DOI : 10.31695/IJERAT.2019.3388

The resulting data was then used to estimate spatial distribution of drought severity using the Krigging estimator in the ArcGIS 10.1. In this study, sixteen hydrometric stations within and adjacent to the upper Tana River basin were used for hydrological evaluation. These stations had unique geographical location and their spatial extent was created through the application GIS. The GIS tool was used to compute and present the spatial distribution, variation and trends of droughts for SMDI.

2.10 Development of Severity-area-frequency (SAF) Curves

The severity-area-frequency (SAF) curves were developed using data on drought severity, area and frequency. A summary of the step by step procedure for development of the curves used in this study is described as:

(i) For each year, the drought severity at each station is assessment using severity equation (6)
(ii) The spatial distribution of the drought severity using ArcGIS 10.1 and the kriging method is estimated
(iii) The drought severity associated with the areal extent in percentage using the spatial distribution map was determined
(iv) The frequency analysis for each drought areal extent to link drought severity with selected return period was conducted
(v) The drought severity-area-frequency (SAF) curves for the basin based on appropriate probability for (iv) were formulated and plotted

3. RESULTS AND DISCUSSIONS

3.1 Time series Soil Moisture Deficit Index (SMDI)

The SMDI monthly series data was grouped into dry and the wet periods for the computed values of SMDI at 60-cm soil depth that represents the most active Plant rooting zone for plant evapotranspiration according to [9]. Analyzing the seasonality of drought required definition of the distinct seasons. The seasonal occurrence of droughts was evaluated by analyzing drought events separated into each season [3]. The dry period includes the months of July to September (J-S) and January to March (J-M) while the wet period includes the months of October to December (O-D) and March to June (M-J). The average SMDI was computed for each season to describe the agricultural drought condition for the upper Tana River basin. From the results given in Figures 5 to 8, it is observed that the seasonal drought magnitudes vary from year to year. Such a trend is consistent with that presented by [25] in Evinos river basin in Greece.

The results also show that the dry seasonal SMDI values in the months of January to March are consistently higher than the ones for July to September. This significant discrepancy between the SMDI values for the months of January to March, and July to September is due to the influence of the normal hydrological regime of the basin manifested as long dry period and short dry period. The time series results of SMDI for dry and wet seasons were compared. Using the meteorological station 9037112 for illustration, it is observed that the values of SMDI for the dry season are consistently lower than those for the wet seasons as given in Figures 5 and 6. From Figures 5 and 7, it is evident that the SMDI time series values for 9037112 located at lower elevations of the basin is less than those for the meteorological station 9037064 which is at higher elevations. Thus, it can be deduced that the areas within the lower elevations are more prone to drought risks than those in the higher elevations.

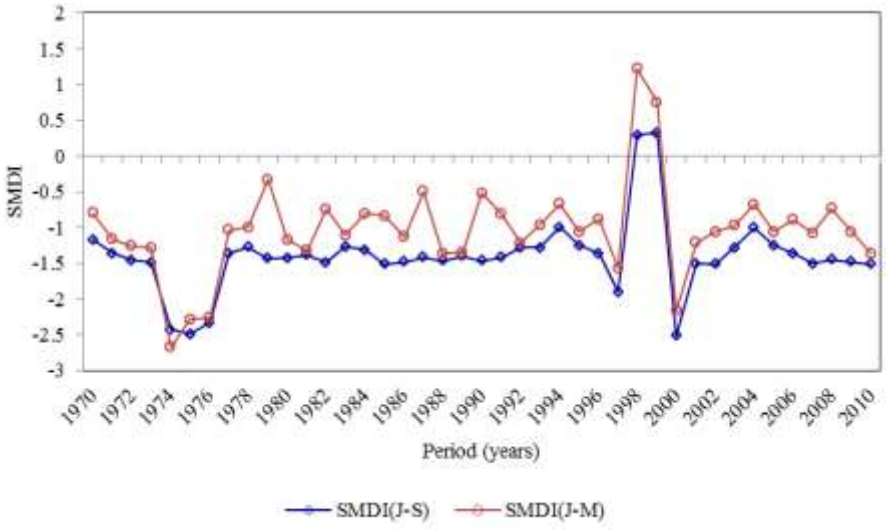

Figure 5: Time series of SMDI for dry season of at MIAD meteorological station

DOI : 10.31695/IJERAT.2019.3388

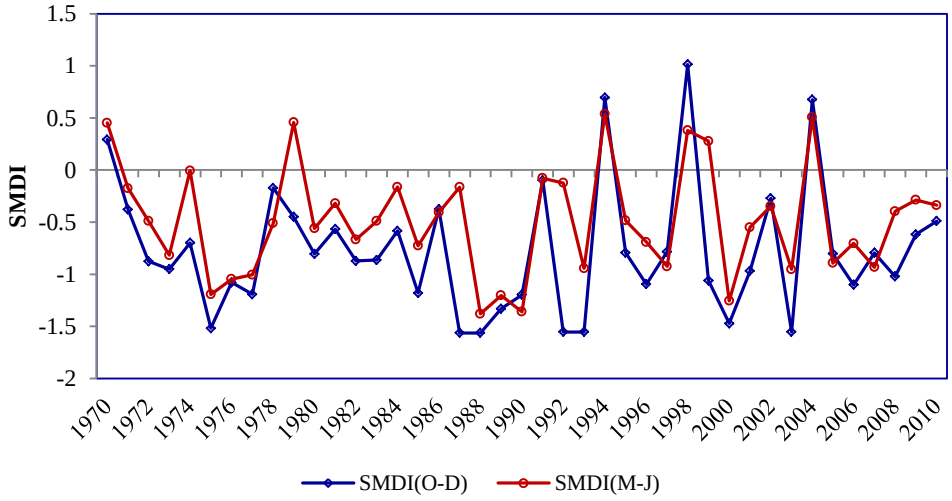

Figure 6: Time series of SMDI for wet season at MIAD meteorological station

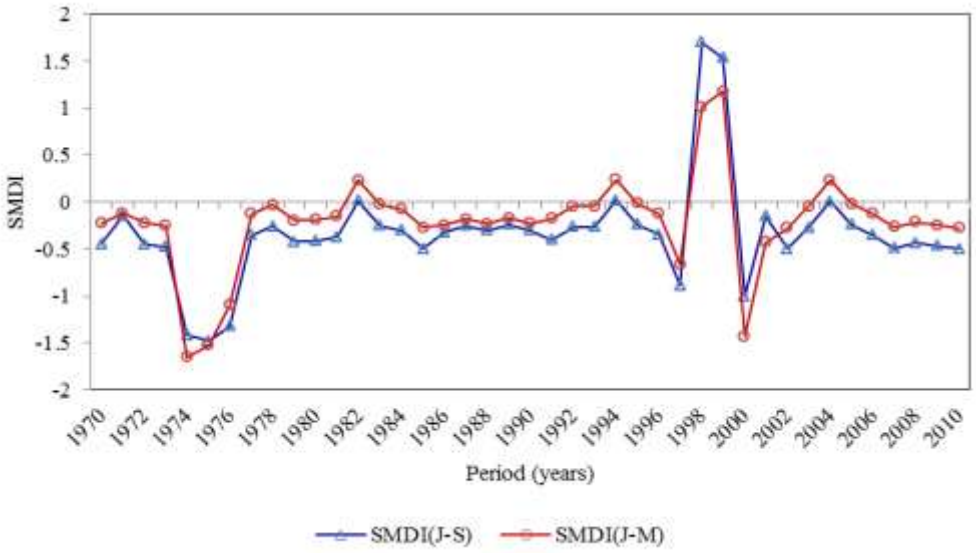

Figure 7: Time series of SMDI for dry season at Naro-moru meteorological station

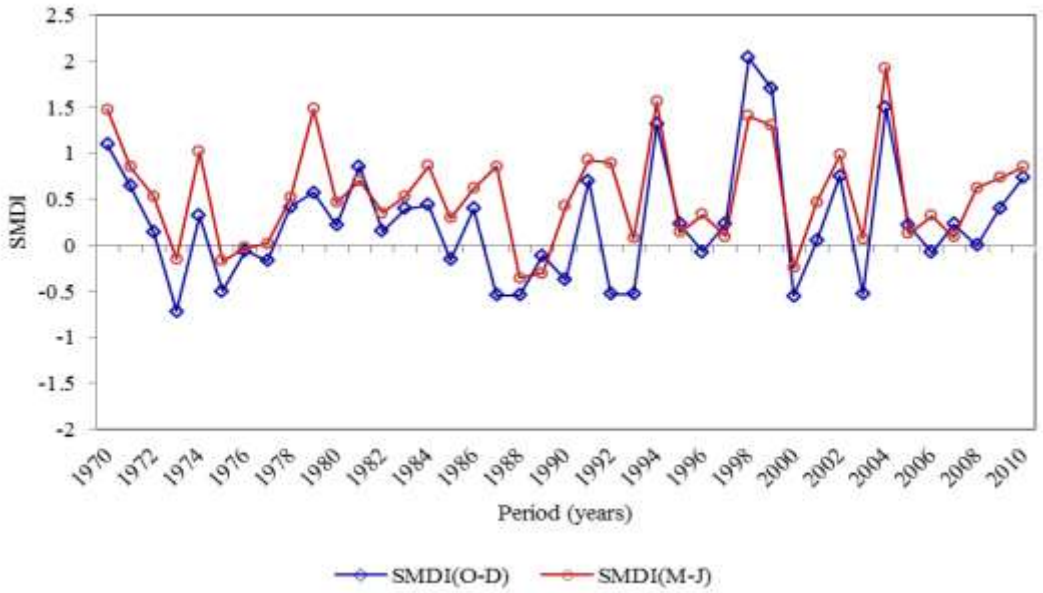

Figure 8: Time series of SMDI for wet season at Naro-moru meteorological station

Based on drought projections of the RMSNN The most notable drought episodes expected for the upper Tana river basin is as presented in Figure 9 at MIAD meteorological station. the projected seasonal droughts severity is as shown in Figure 9 and 10.

DOI : 10.31695/IJERAT.2019.3388

The drought severity values from the figure can be categorized into extreme (less than -2.00), severe(-1.5 to -1.99), moderate (-1.0 to -1.49), near normal(-0.99 to 0.99), moderately wet (0.7 to 1.49), very wet(1.50 to 2.49) and extreme wet (2.5 or more) drought conditions for future agricultural planning.

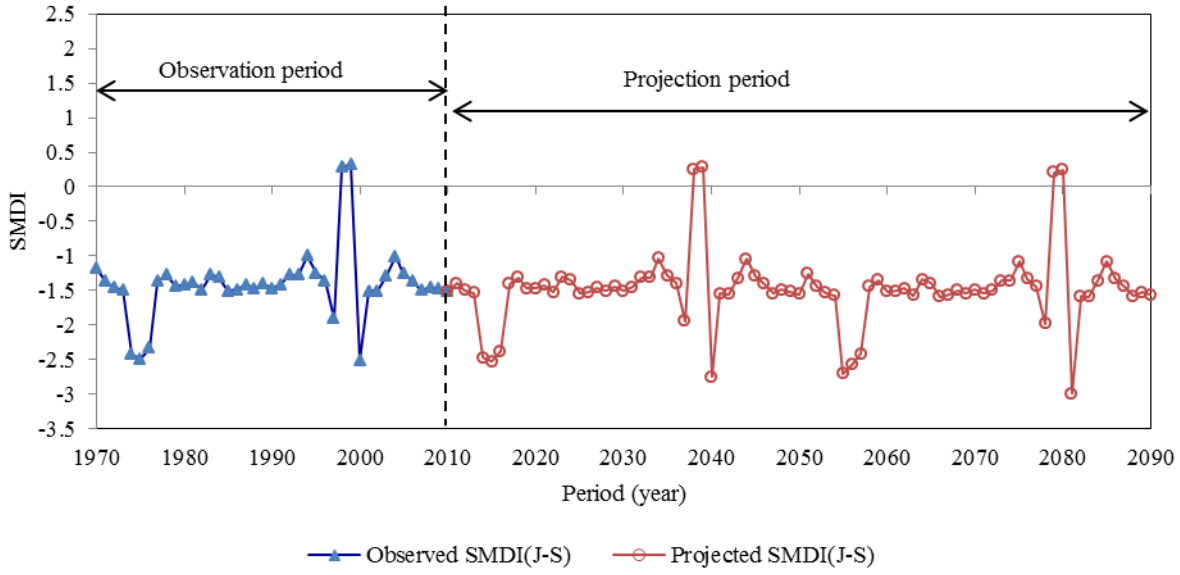

Figure 9. Observed and projected drought at MIAD s meteorological tation

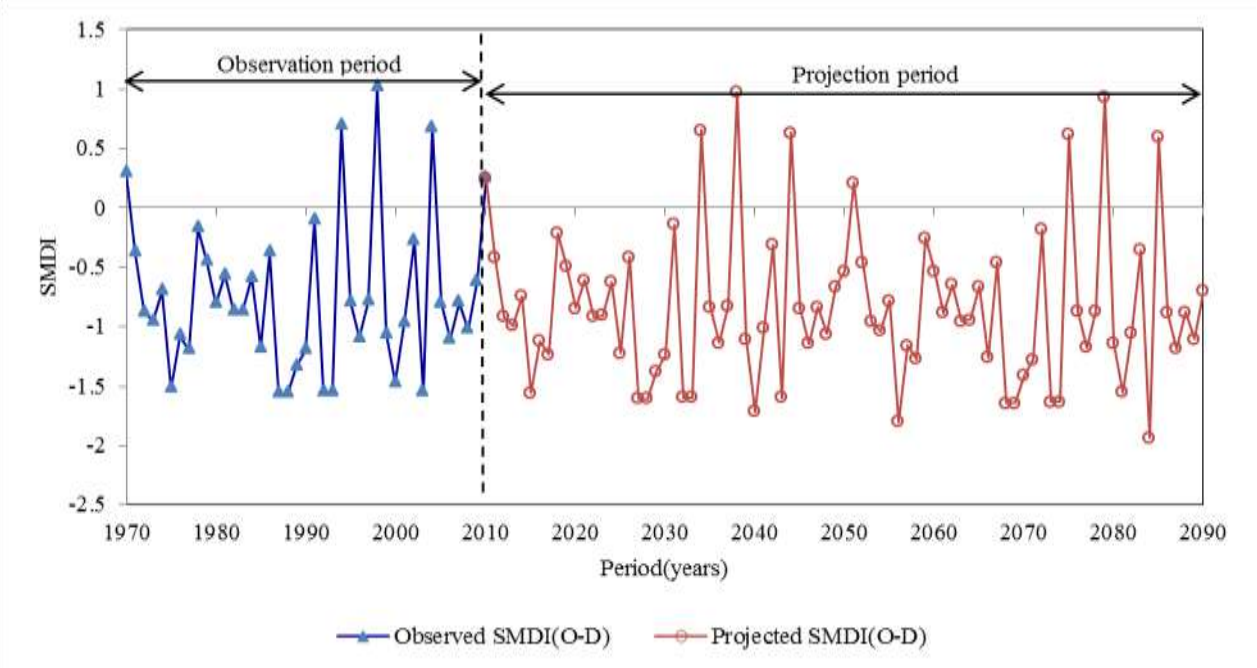

Figure 10. Observed and projected drought at Naro-moru meteorological station

3.2 Spatially distributed drought severity based on SMDI

The results of SMDI spatial distribution of drought as presented in Figure 8 show that the minimum and maximum drought severity values in 1970 are from -0.661 to 0.603 and 0.807 to 0.769 respectively. These drought severities are experienced in the north-western and south-eastern areas of the basin as given in Figure 11a. From the results given in Figure 11c, it is observed that the values increased from -0.715 to -0.658 and -0.886 to -0.829 between 1970 and 2010. This is an indication that the south-eastern parts of the basin are the most susceptible to droughts as detected by the SMDI while the north-western areas are least prone to droughts.

DOI : 10.31695/IJERAT.2019.3388

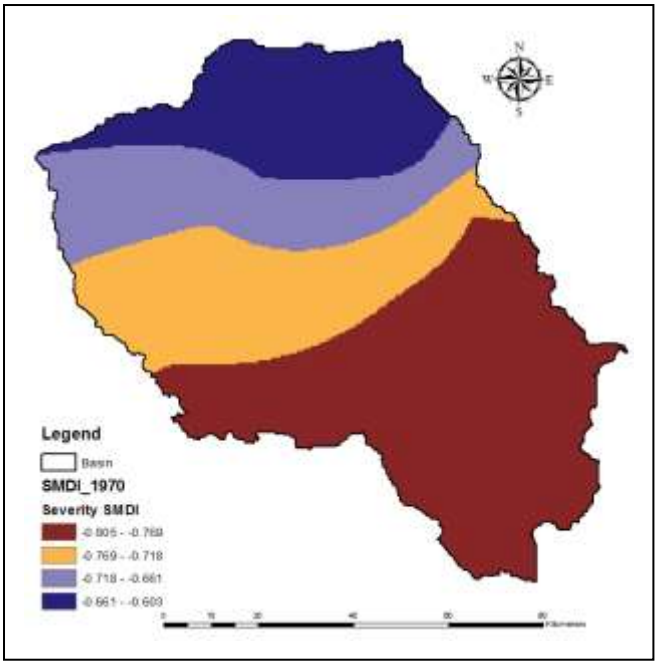

(a)

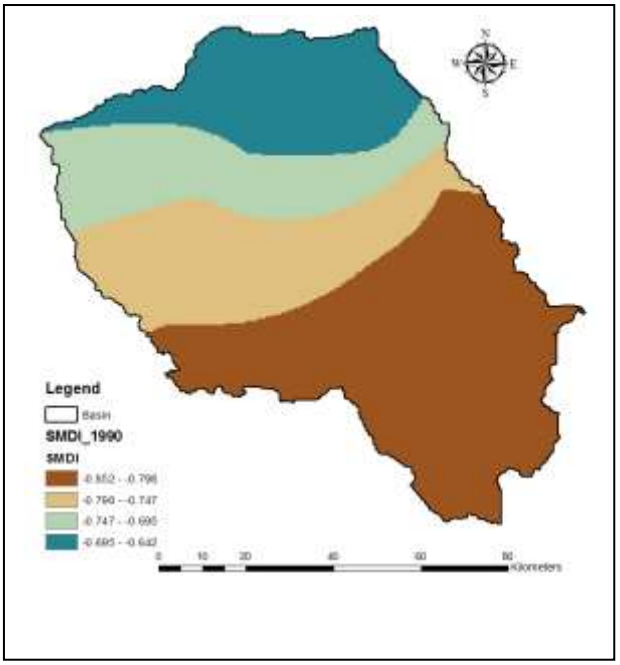

(b)

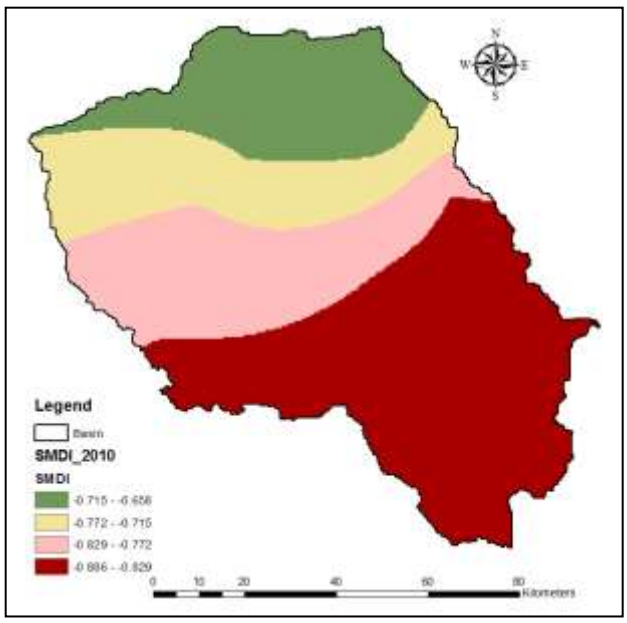

(c)

Figure 11 (a-c): Spatially distributed drought severity based on SMDI

Figure 12 shows how the SMDI has changed over the 41 year period for both south-eastern and north-western areas of upper Tana River basin. The SMDI changed from -0.625 to – 0.725 while that of north-western parts changed from -0.795 to -0.895. For both areas, the gradient of the two curves that illustrate the rate of increase of drought for the period exhibit an increase of -0.003 per year. This means that the gradient can be used to project the SMDI values for future years.

DOI : 10.31695/IJERAT.2019.3388

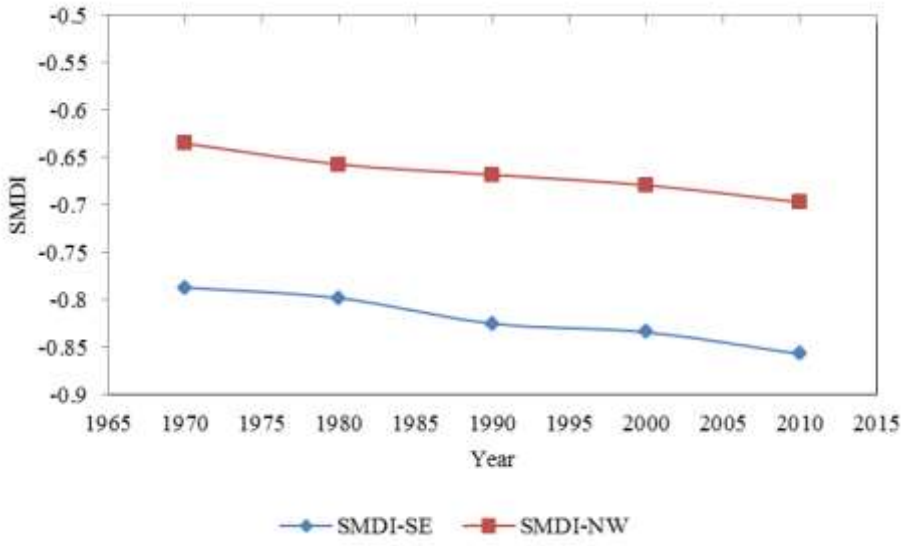

Figure 12: The trend of SMDI over the 1970-2010 period

Drought in the upper Tana River basin is explained using the severity-area-frequency curves constructed for the basin (Figure 13).

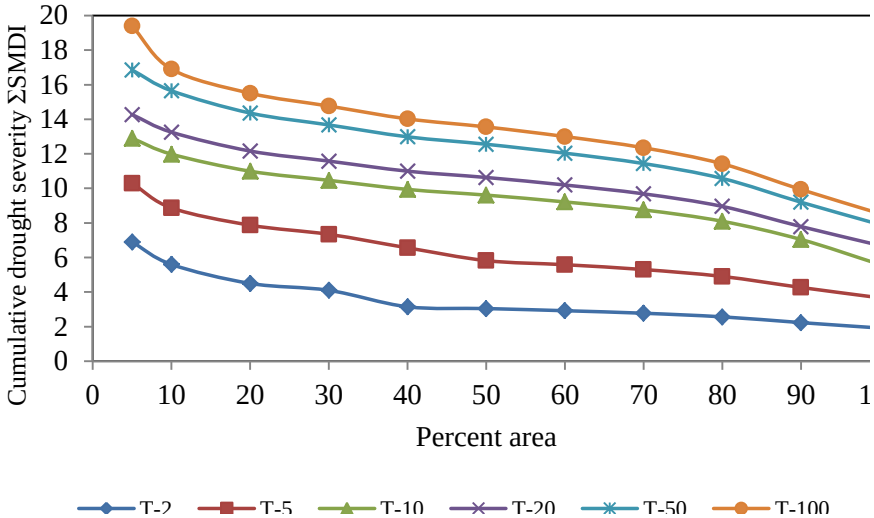

Figure 13: The Severity-area-frequency (SAF) curves based on SMDI

According to the analysis of the SAF curves the drought severity area frequency relationship can be analysed. For any return period, the higher the drought severity, the lower the areal extent. For instance for a 5 year (T-5) return period, a drought severity of 10 correspond to an area of 5 per cent (871 km^2) while a severity of 5 correspond to 90 per cent (15678 km^2) areal extent. A drought severity of 5.5 has an areal coverage of 5 per cent for a 2-year (T-2) return period. However, the 5 per cent area corresponds to a cumulative drought severity of 18.5 for a 100-year (T-100) return period. On the other hand a drought severity of 2.5 has an areal coverage of 95 per cent (16549 km^2) for a 2-year (T-2) return period while this 95 percent areal extent correspond to drought severity of 8 for a 100-year (T-100) return period (Figure 10).

4. CONCLUSION

From the results of spatial characterization of drought, it is deduced that for upper Tana River basin, the areas within the lower elevations are more prone to drought risks than those in the higher elevations. The south-eastern parts of the upper Tana River basin are the most susceptible to droughts as detected by the SMDI while the north-western areas are least prone to the droughts. The temporal series results of SMDI for dry and wet seasons for all meteorological stations show that the drought is more severe during dry periods than wet seasons. The drought projection can be adopted for planning ahead for mitigation and adaptation of adverse effects of droughts on agriculture and formulate food security programs in the river basin.

Acknowledgement

Author(s) acknowledge the African Development Bank (AfDB) for a doctoral scholarship offered that culminated to this manuscript. The authors are grateful for the scholars whose articles and books are cited and or include in this manuscript. In addition, the authors appreciate the editors and publishers of all the articles, journals and books used in this text. Authors are grateful to the editors of the journal that accept to publish this manuscript for its access by other readers.

DOI : 10.31695/IJERAT.2019.3388

REFERENCES

[1] Barua, S. (2010). Drought assessment and forecasting using a non-linear aggregated drought index, PhD thesis, Victoria University, Australia.

[2] Belayneh, A. and Adamowski, J. (2013). Drought forecasting using new machine learning methods, *Journal of Water and Land Development*, 18 (I-IV): 3-12.

[3] Birkel, C. (2005). Temporal and spatial variation of drought indices in Costa Rica, MSc thesis, Istitut für Hydrologie, der Albert-Ludwigs-Universität Freiburg i. Br.

[4] Bonacci, O. (1993). Hydrological identification of drought, hydrological processes, 7: 249-262.

[5] Casa, A., Ovando, G., Bressanini, L. and Martinez, J. (2013). Aquacrop model calibration in potato and its use to estimate yield variability under field conditions, *Atm and Clim sciences*, 3: 397-407.

[6]Castano, A. (2012). Monitoring drought at river basin and regional scale: application in Sicily, PhD Dessertation in Hydraulic Engineering, University of Catania, Italy.

[7] Dracup, J. A., Lee, K. S. and Paulson, E. G. (1980a). On the statistical characteristics of drought events, *Journal of water resources research*, 16(2): 289-296.

[8] Du, W., He, X., Shamaila, Z., Hu, Z., Zeng, A. and Muller, J. (2011). Yield and biomass prediction testing of AquaCrop model for winter wheat, *transactions of the Chinese society of agricultural machinery*, 42: 174-178.

[9] FAO. (2013). Report on land and water, www.fao.org/nrl/aboutnr/nrl, accessed on 5th February, 2014.

[10] Fiseha, B. M., Setagn, S. G., Melesse, A. M., Volpi, E. and Fiori, A. (2013). Hydrological analysis of the upper Tiber river basin, central Italy: A watershed modelling approach, *Hydrological processes*, 27:2339-2357.

[11] IFAD. (2012). Upper Tana catchment natural resource management project report, east and southern Africa division, project management department.

[12] Iqbal, M. A., Shen, Y., Stricevic, R., Pei, H., Sun, H., Amini, E., Penas, A. and Rios, S. (2014). Evaluation of the FAO AquaCrop model for winter wheat on the north China plain under deficit irrigation from field experiments to regional yield simulation, *Agricultural Water Management Journal*, 135(2014): 61-72.

[13] Jacobs, J. Angerer, J., Vitale, J., Srinivasan, R., Kaitho, J. and Stuth, J. (2004). Exploring the Potential Impact of Restoration on Hydrology of the Upper Tana RiverCatchment and Masinga Dam, Kenya, a Draft Report, Texas A & M University.

[14] Kang, S., Zhang, L. and Trout, T. (2017). Improving agricultural water productivity to ensure food security under changing environment, special issue –*Agricultural water management*, 179: 1-4.

[15] Karamouz, M. Rasouli, K. and Nazi, S. (2009). Development of a hybrid index for drought prediction: case study, *Journal of Hydrologic Engineering*, 14(6): 617-627.

[16] Karamouz, M., Szidarovszky, F. and Zaharaie, B. (2003). Water resources systems analysis, Lewis Publishers, Florida, U.S.A

[17] Karl, T. R. and Knight, R. W. (1985). Atlas of monthly palmer hydrological drought indices for the continuous United States, Asheville, N.C USA national climatic data centre, climatology series (3-7) report.

[18] Loucks, D. P. and van-Beek, E. (2005). Water resources systems planning and management, an introduction to methods, models and applications, studies and reports in hydrology, UNESCO publishing Paris.

[19] Manikandan, M. and Tamilmani, D. (2013). Development of drought vulnerability maps in the Parambikulam-Alyar Basin, India, *Academic Journals*, 8(20): 778-790.

[20] Mishra A. K. and Dessai V. R. (2006). Drought forecasting using feed-forward recursive neural networks, *Journal of ecological modelling*, 198: 127-138.

[21] Mishra, A. K. and Singh, V. P. (2010). A Review of Drought Concepts, *Journal of Hydrology*, 391 (1-2): 202-216.

[22] Morid, S. Smakhtin, V. and Bagherzadeh, K. (2007). Drought forecasting using artificial neural networks and time series of drought indices *International Journal of climatology*, 27 (15): 2103-2111.

[23] Mulla, D. (2013). Twenty five years of remote sensing in precision agriculture: key advances and remaining knowledge gaps, *Journal of Biosystems Engineering*, 114 (4): 358-371.

[24] Mutua, B. M. and Klik, A. (2007). Predicting daily stream flow in un-gauged rural catchments; the case of upper Tana River basin, Kenya, *Journal of spatial hydrology*, 5(2): 64-80.

[25] Nalbantis, I. (2008). Evaluation of hydrological drought index, *European water journal*, 23(24): 67-77.

[26] Narasimhan, B. and Srinivasan, R. (2005). Development and evaluation of soil moisture deficit (SMDI) and evapo-traspiration deficit index (ETDI) for agricultural drought monitoring, *Journal of agricultural and forest meteorology*, 133: 69-88.

[27] Narasimhan, B. and Srinivasan, R. (2005). Development and evaluation of soil moisture deficit (SMDI) and evapo-traspiration deficit index (ETDI) for agricultural drought monitoring, *Journal of agricultural and forest meteorology*, 133: 69-88.

[28] NEMA. (2004). Kenya state of environment report: Chapter 7, fresh water, coastal and marine resources, Nairobi, Government printer.

[29] Otieno, F. A. O. and Maingi, S. M. (2000). Sedimentation problems of Masinga reservoir. In land and water management in Kenya. Eds. Gichuki F. N., Mungai, D. N., Gachere, C. K. and Thomas, D. B., published by Soil and Water Conservation branch of Ministry of Agriculture and Rural development, Nairobi, Kenya.

[30] Palmer, W. C. (1965). Meteorological drought research paper 45, weather Bureau, Washington D.C, U.S.A.

[31] Ramazani, E. H., Liaghat, A., Parsinezhad, M. and Ramazani, E. M. (2012). The study of agriculturl drought on soil moisture in Qazvin station, *Journal of water in agriculture*, 2(1): 84-93.

[32] Saenyi, W. W. (2002). Sediment management in Masinga reservoir, Kenya, PhD thesis (Published), University of Agricultural Sciences (BOKU), Vienna Austria.

[33] Sanchez, N, Gonzalez-zamora, A., Piles, M., and Martinez-ferranchez, J. (2016). A new soil moisture agricultural drought index (SMADI) integrating MODIS and SMOS products: a case study over the Iberian Peninsula, *remote sensing journal* 8(4) 287-312.

DOI : 10.31695/IJERAT.2019.3388

[34] Sayanjali, M. and Nabdel, O. (2013). Remote sensing satellite design using model based systems Engineering, *Journal of Science and Engineering*, 1(1): 43-54.

[35]Sivapravasam, S. Murugappan, A. and Mohan, S. (2011). Modified Hargreaves Equation for estimation of ETo in a hot and humid location in Tamilnadu state, India, *International journal of Engineering Science and Technology*, 3(1): 592-600.

[36] Shuaibu, S. M., Ogbodo, J. A., Wasige, E. J. and Mashi, S. A. (2016). Assessing the impact of agricultural drought on maize prices in Kenya with approach of the SPOT-VEGETATION NDVI remote sensing, *International journal of remote sensing* 28(7): 1503-1524.

[37] Tsakiris, G. and Nalbantis, I. (2009). Assessment of hydrological drought revised, *water resources management*, 23: 881-897.

[38] Wang, W. (2010). Drought analysis under climate change by application of drought indices and copulas, MSc thesis in Civil and Environmental Engineering, Portland State University.

[39] Wilschut, L. I. (2010). Land use in the upper Tana: Technical report of a remote sensing based land use map. In green water credits report 9 edited by Mcmillan B., Kauffmann, S. and De Jon, R. Wageningen, ISRIC-world soil information.

[40] World Resources Institute (WRI). (2011). Kenya GIS data –world resources institute, retrieve from www.wri.org/resources/data-sets/kenya-gis-data on January 15, 2014.

[41] Yan, D. H., Wu, D., Huang, R., Wang, L. R. and Yang, G. Y. (2013). Drought evolution characteristics and precipitation intensity changes during alternating dry-wet changes in Huang-Huai-Hai River basin, *Journal of Hydrology and Earth Systems Sciences*, 10: 2665-2696.

[42] Yan, D., Shi, X., Yang, Z., Li, Y., Zhao, K. and Yuan, Y. (2013). Modified palmer drought severity index based on distributed hydrological simulation, *Journal of mathematical problem in Engineering*, 2013: 1-8.

[43] Zoljoodi, M. and Didevarasl, A. (2013). Evaluation of Spatio-temporal variability of droughts in Iran using Palmer Drought Severity Index and its precipitation factors through (1951-2005), *Atmosphere and Climate Sciences Journal*, 3: 193-207.

DOI : 10.31695/IJERAT.2019.3388